J Nondestruct Eval (2013) 32:294–299
DOI 10.1007/s10921-013-0182-z

Fast Analytical Modeling of Eddy Current Non-Destructive Testing of Magnetic Material

T. Bouchala · B. Abdelhadi · A. Benoudjit

Received: 30 January 2013 / Accepted: 17 May 2013 / Published online: 31 May 2013

Abstract This article presents the modeling of non-destructive testing systems containing magnetic materials using a fast numerical method. Its main aim consists of correcting the half analytical expression of the impedance variation, formulated by some authors, caused by the presence of a conducting plate below of an absolute ferrite core probe. The obtained results of this correction are found to be consistent and satisfactory comparatively to those of finite element method. It also deals with the study the method rapidity by comparing its simulation time to that of the finite element method. As result, the proposed method is found to be very fast and a very short simulation time is required to calculate the sensor impedance. Indeed, for the studied system the coupled circuit simulation time is lower than 1.09 s. This study is appreciable, since it permits to solve quickly the inverse problem by expressing the physical and geometrical features of the material or defect according to the measured parameters. More importantly, this method is applicable to any axi-symmetric systems and can be adapted for the simulation of three-dimensional configurations.

Keywords Ferrite core probe · Eddy current · Fast analytical modeling · Non-destructive testing

1 Introduction

Since its appearance, the coupled circuit method (CCM) has been used for eddy current non-destructive testing (EC-NDT) modeling of non-magnetic materials [1–6]. Many authors have elaborated the modeling of magnetic materials regardless of their actual physical properties such as electrical conductivity and magnetic permeability. In the study carried out in [7], the interaction between the ferromagnetic core and the material to be tested is neglected and the variation in equivalent fictitious currents is not taken into account in the expression of the impedance variation caused by the presence of a piece or defect. Therefore, this study consists chiefly of completing the expression of ferrite core coil impedance by introducing the term that expresses the interaction between the ferrite core and the controlled piece [8]. On the other hand, in order to demonstrate the rapidity of the proposed model, a quantitative study is carried out by comparing its simulation time to that of the finite element method. As result, for the standard frequencies generally used in EC-NDT [7], the proposed method is found to be very fast and a very short simulation time is sufficient to calculate the sensor impedance. Generally, the target of such development of the forward models is to elaborate fast and accurate inversion methods that permit a full characterizing of materials or defect in real time [9]. Indeed, the developed model is very important because it is very fast and allows expressing the ferrite core coil impedance according to the controlled pieces characteristics; hence the inversion procedure becomes easier when the measured quantities are known.

T. Bouchala (✉)
Electrical Engineering Department, University El-Hadj Lakhdar, Batna, Algeria
e-mail: buizra@yahoo.fr

B. Abdelhadi · A. Benoudjit
Electrical Engineering Department, Laboratory of Electric Traction Systems (LSTE), El-Hadj Lakhdar University, Batna, Algeria

B. Abdelhadi
e-mail: abdelhadi3b@yahoo.com

A. Benoudjit
e-mail: benoudjit@yahoo.fr

2 Notion of equivalent sources of magnetization

The method consists in replacing the magnetic environment on which the calculation of the field is fulfilled by a non magnetic one with the equivalent distribution in currents [7]. If $\vec{M}$ is the magnetization, we have:

$$\vec{J}_V = \vec{rot}\vec{M} \quad (1)$$

$$\vec{J}_s = (\vec{M} \times \vec{n}) \quad (2)$$

where: $\vec{J}_V$ is fictitious current density, flowing inside the volume, due to the volume material magnetization. $\vec{J}_s$ is fictitious current density, flowing on the surface, due to the surface material magnetization.

In the case of a linear homogeneous ferrite, if its electric conductivity is neglected, the volume current will also be neglected. As the currents spreads only on the surface, they are expressed by the second equation of Fredholm as follows:

$$\frac{\mu_o}{2}\frac{1+\mu_r}{1-\mu_r}J_m^{(m)} - \vec{n} \times \vec{B}^{(m)} = \vec{n} \times \vec{B}^{(o)} \quad (3)$$

where: $\vec{B}^{(m)}$ is magnetic induction created by the superficial fictitious current I_m. $\vec{B}^{(o)}$ is magnetic induction created by the current of the source I_o.

These induction densities are expressed by the relations deducted from Biot and Savart law, as expressed below:

$$\vec{B}(p) = \frac{\mu_o}{8\pi}\int^{\Omega}\big[Gbr(p,p_s)\vec{e}_r + Gbz(p,p_s)\vec{e}_z\big]J(p_s)d\Omega \quad (4)$$

where p and p_s are the receptive and the source points respectively and $J(p_s)$ is the current density corresponding to this point p_s.

Gbr and Gbz are the functions of receptive point $p(r,z)$ and the source point $p(r_s,z_s)$, [7].

$$Gbr(p,p_s) = \frac{z-z_s}{r}\frac{k}{\sqrt{rr_s}}\left[\frac{2-k^2}{1-k^2}E_2(k) - 2E_1(k)\right] \quad (5)$$

$$Gbr(p,p_s) = -\frac{k}{\sqrt{rr_s}}\left[\frac{2-(1+\frac{r_s}{r})k^2}{1-k^2}E_2(k) - 2E_1(k)\right] \quad (6)$$

where $E_1(k)$ and $E_2(k)$ are the 1st and 2nd kind elliptic functions.

$$k(p,q) = \sqrt{\frac{4rr_s}{(r+r_s)^2+(z-z_s)^2}} \quad (7)$$

In order to simplify the equations, we define a gradient of the function such as:

$$\vec{grad}Gb(p,p_s) = Gbr(p,p_s)\vec{e}_r + Gbz(p,p_s)\vec{e}_z \quad (8)$$

3 Discrete System Description

Practically, in eddy current non-destructive testing (EC-NDT), a better coupling between the sensor and the piece to be tested is often assured by a core of ferrite because it focuses on the magnetic flux into certain area of the specimen so as to increase the probe sensitivity [10–12]. The studied discrete system is depicted in Fig. 1. It composes of a ferrite core sensor and the piece. This figure shows the mesh of its different regions following the two axes. The coil is composed of N_o turns disposed in series: N_{oz} elements following the vertical axis and N_{or} elements following the horizontal axis. The piece (Ω_o) is subdivided into N_c circular elements representing the elementary turns arranged in parallel: N_{cz} according to the vertical axis and N_{cr} elements according to the horizontal axis. When neglecting the fictitious currents of ferrite volume, the meshing will concern only the ferrite cored surface (Γ_m), N_{mz} elements according the vertical axis and N_{mr} following the radial axis.

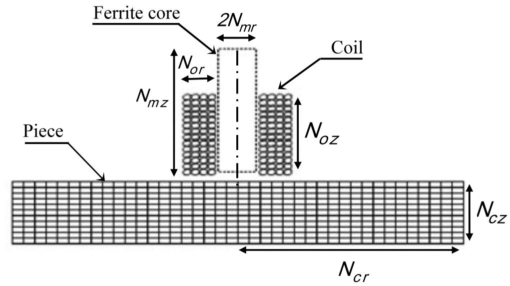

Fig. 1 Discrete system of electromagnetic sensor and tested piece

This system is in symmetry of revolution, therefore only one half of domain will be studied. Indeed, while taking into account this subdivision, we get the following system:

$$\begin{cases} N_c = N_{cr}N_{cz} \\ N_o = N_{or}N_{oz} \\ N_m = 2N_{mr} + N_{mz} \end{cases} \quad (9)$$

The elementary sections and linear element are given as follows:

$$\begin{cases} s_c = \dfrac{\Omega_c}{N_c} \\ s_o = \dfrac{\Omega_o}{N_o} \\ l_m = \dfrac{\Omega_m}{N_m} \end{cases} \quad (10)$$

Such an eddy current sensor relies on the sensor impedance variation to perform the measurement of physical parameters, and the sensor impedance is an important parameter for investigating the properties of an eddy current sensor [13]. Therefore, the calculation approach of this impedance is very important. In the following investigation, preserving the previous mesh, a semi numerical expression of ferrite core coil impedance variation (difference between the impedance in presence of the load and the impedance in free space) will be developed.

4 Impedance in Free Space

In absence of the load, the sensor impedance is obtained from the both equations in source and ferrite core as expressed hereafter.

4.1 Equation in the Source

To establish the equations in the source, in the piece and in the ferrite core, we assign to each of these elements the letters (o), (c) and (m) respectively. Also, we designate two points (p) and (q) belonging to the source, (l) and (k) belonging to the piece and (m), (n) belonging to the ferrite core. In absence of the piece, we note by $U^{(a)}$ and $I_m^{(a)}$ the applied voltage and fictitious induced current in the ferrite core respectively. Taking into account the previous mesh, the generalized equation of the coupled electric circuits expressed in [1] and [3], becomes:

$$\sum_{p=1}^{N_o}\frac{2\pi(p)}{\sigma_o(p)s_o(p)}I_o + jI_o\mu_o\omega\sum_{p=1}^{N_o}r(p)\sum_{q=1}^{N_o}G_{oo}(p,q) + j\mu_o\omega\sum_{p=1}^{N_o}r(p)\sum_{q=1}^{N_o}G_{om}(p,m)I_m^{(a)} = U^{(a)} \tag{11}$$

with: $p = 1, \ldots, N_o$

$\sigma_o(p)$ and $s_o(p)$ are successively the electric conductivity and the section of the turn p belonging to the source.

4.2 Equation in the Ferrite Core

In the ferrite core, the electric conductivity is neglected, therefore, only the superficial current exists. Considering transformation (7), (3) becomes:

$$\frac{\mu_o}{2}\frac{1+\mu_r}{l_m(m)(1-\mu_r)}I_m^{(a)}(m) - \frac{\mu_o}{8\pi}\sum_{n=1}^{N_m}\vec{n}\times gr\vec{a}dG_{mm}(m,n)I_m^{(a)}(n) = \frac{\mu_o}{2}I_o\sum_{p=1}^{N_o}\vec{n}\times gr\vec{a}dG_{mo}(m,p) \tag{12}$$

with: $m = 1, \ldots, N_m$.

4.3 Coil impedance in free space

The ferrite core coil impedance Z_o is defined as the ratio between the voltage $U^{(a)}$ and the feeding current I_o. If we note by Z_b the coil impedance, from (11), the one in free space can be expressed as follows.

$$Z_o = Z_b + \frac{j\mu_o\omega}{I_o}\sum_{p=1}^{N_o}r(p)\sum_{m=1}^{N_m}G_{om}(p,m)I_m^{(a)}(m) \tag{13}$$

5 Coil Impedance Expression in Presence of the Load

In presence of the load, the coil impedance is expressed in the same manner as in the above case (in free space) while considering the load induced current (I_c) effect, as follows.

5.1 Equation in the Source

In this case, we introduce the effect of the eddy currents (I_c) in the piece. Similarly, in presence of the load, we note by $U^{(c)}$ and $I_m^{(c)}$ the applied voltage and fictitious current in the ferrite core respectively. Then, (11) becomes:

$$\sum_{p=1}^{N_o}\frac{2\pi(p)}{\sigma_o(p)s_o(p)}I_o + jI_o\mu_o\omega\sum_{p=1}^{N_o}r(p)\sum_{q=1}^{N_o}G_{oo}(p,q) + j\mu_o\omega\sum_{p=1}^{N_o}r(p)\sum_{m=1}^{N_m}G_{om}(p,m)I_m^{(c)}(m) + j\mu_o\omega\sum_{p=1}^{N_o}r(p)\sum_{k=1}^{N_c}G_{oc}(p,k)I_c = U^{(c)} \tag{14}$$

with: $p = 1, \ldots, N_o$.

5.2 Ferrite Core Coil Impedance Expression

Using (13), the ferrite-cored coil impedance Z is expressed in presence of the piece by the following equation.

$$Z_o = Z_b + \frac{j\mu_o\omega}{I_o}\sum_{p=1}^{N_o}r(p)\sum_{m=1}^{N_m}G_{om}(p,m)I_m^{(c)}(m) + \frac{j\mu_o\omega}{I_o}\sum_{p=1}^{N_o}r(p)\sum_{k=1}^{N_c}G_{oc}(p,k)I_c(k) \tag{15}$$

6 Impedance Variation Due to the Piece Presence

The impedance variation due to the piece presence is obtained by subtracting the impedance in free space Z_o from that in the load Z.

$$\Delta Z = Z - Z_o \tag{16}$$

It is given by the following expression:

$$Z_o = \frac{j\mu_o\omega}{I_o}\sum_{p=1}^{N_o}r(p) \times\left(\sum_{m=1}^{N_m}G_{om}(p,m)\left(\frac{I_m^{(c)}(m)-I_m^{(a)}(m)}{I_o}\right)\right) + \frac{j\mu_o\omega}{I_o}\sum_{p=1}^{N_o}r(p)\sum_{k=1}^{N_c}G_{oc}(p,k)I_c(k) \tag{17}$$

This impedance model takes into consideration all inductive phenomena that are not taken into account in previous works such as that of [7], where the impedance variation is only expressed in function of the load parameters. Equation (17) shows that the impedance variation is not only function of the load parameters, but it is also affected by the interaction between the ferrite core and the load [8]. In other terms, the literature published models suppose that $I_m^{(a)} = I_m^{(c)}$, however our simulation results demonstrate that this assumption is not accurate and hence the results with this assumption are relatively affected.

7 Quantitative Comparison Between Finite Element and Coupled Circuit Methods

In order to quantify the proposed model of non-destructive control, we treat the axi-symmetrical configuration given in Fig. 2 [14].

The geometrical and physical characteristics are given in Table 1.

In absence of the ferrite core, the simulation is implemented in a personnel computer (PC) with CPU frequency of 2 GHz and a RAM of 3 GB. For this configuration, the impedance values are calculated by the proposed model of coupled circuit method (CCM) and compared to those of Finite Element Method (FEM) as reported in Table 2.

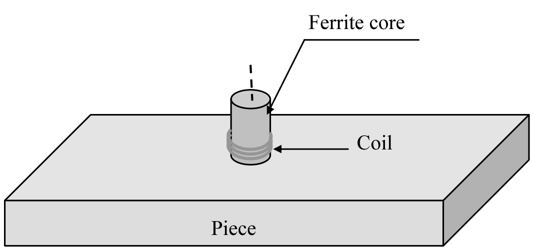

Fig. 2 Geometrical configuration of the treated system

As can be noted from Table 2, the average value of relative errors (ΔZ) between the impedance calculated by the proposed model and that of FEM do not exceed 2.83 %. Therefore, according to these small errors which reveal that the results are in good concordance and the adopted model is well validated.

According to the simulation times reported in Table 2, we can confirm that the coupled circuit method is very quick and faster than finite element method (for the studied system the CCM simulation time is lower than 1.09 s). Although the CCM mesh is regular following the two axes, contrary to the FEM mesh that is generated irregularly by Matlab software (optimized mesh).

The distribution of induced currents I_c in the plate, calculated by CCM, is illustrated in Fig. 3.

Figure 3 shows clearly that the induced currents Ic are important in the neighboring zone of the coil. On the other hand, they decrease in amplitude according to the depth of the plate. The depth of penetration (for the standard frequencies) is less than its thickness, while taking into account the previous considerations; we can elaborate an irregular mesh following the two axes. Consequently, the simulation time will be considerably reduced.

8 Validation of the Corrected Impedance Expression

Expression (17) explains clearly that the magnetization in ferrite core is influenced by the presence of the piece ($I_m^{(c)} \neq$

Table 1 Geometrical and physical characteristics of the system

Coil		Ferrite core		Piece	
High	6.3500 mm	High	12.7 mm	Lift-off	0.1 mm
Inner radius	1.5875 mm	Radius	1.5875 mm	R_{max}	12 mm
Outer radius	3.1750 mm	Magnetic permeability	1000	Electric conductivity	35 MS/m
Number of spires	16				
Electric conductivity	59.6 MS/m				

Table 2 Impedance relative difference and simulation time obtained using the proposed coupled circuit model (CCM) and finite element method (FEM)

Frequency	1 MHz	100 KHz	10 KHz
Depth of penetration (mm)	0.085	0.27	0.85
Impedance Z with FEM (Ω)	$0.026 + 2.36j$	$0.011 + 0.24j$	$0.007 + 0.025j$
Simulation time T_f (s)	1.60	1.45	1.30
Impedance Z with CCM (Ω)	$0.022 + 2.32j$	$0.010 + 0.23j$	$0.007 + 0.024j$
Simulation time T_c (s)	1.09	0.32	0.11
Impedance relative error (%)	1.7	3.1	3.7

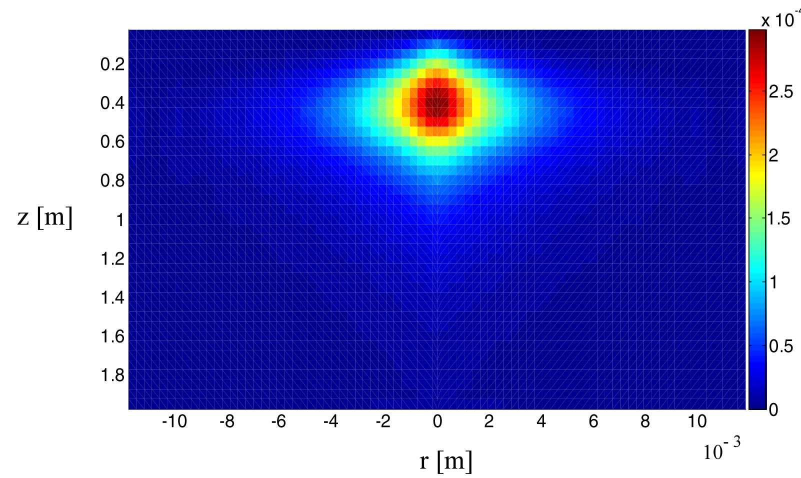

Fig. 3 Distribution of induced currents Ic (A) in the section of the plate, calculated with CCM, $f_r = 10$ KHz

Table 3 Normalized impedances calculated by FEM and CCM

Frequency	1 MHz	100 KHz	1 KHz
Zn with FEM (Ω)	0.011 + 0.63j	0.025 + 0.67j	0.090 + 0.87j
Zn with CCM (Ω)	0.012 + 0.64j	0.026 + 0.68j	0.093 + 0.89j
Impedance relative error (%)	1.6	1.5	2.3

$I_m^{(a)}$) and the impedance variation is also affected. In previous contributions such as that of [7], the impedance variation is only expressed in function of the load parameters (the second term of (17)). This is not reasonable, and our simulation results demonstrate that this assumption is not accurate and hence the results with this assumption are relatively affected. Indeed, this expression must be completed by introducing the first term of (17).

To demonstrate the accuracy of the improved semi numerical expression, we take the same configuration treated previously, but in this case the coil is equipped by a ferrite core of magnetic permeability $\mu_r = 1000$. The normalized impedance calculated using FEM and the proposed CCM is given on Table 3.

From Table 3, we remark that the relative difference between the normalized impedance calculated by the proposed model and that of FEM do not exceed 2.3 %.

Furthermore, this study has led to a number of characteristics. Figures 4, 5 and 6 depict the evolution of the ferrite core fictitious equivalent current. Figures 4 and 5 illustrate respectively the fictitious current on the upper and the lower surfaces. The lateral surface current is represented in Fig. 6.

Figures 4 and 5 demonstrate that the radial fictitious current is maximal on core surface and decreases while approaching the symmetry axis. Figure 6 illustrates that the currents on the vertical surface are important in the coil environment and decreases while moving away from it.

9 Conclusion

The eddy current non-destructive testing exploits the electromagnetic induction phenomena. Different analytic and numeric methods are used for the modeling of these devices. Analytical solutions yield closed form expressions of fields but are available only in very simple geometries cases [15, 16]. Nonetheless, numerical methods are precise and applicable to any configurations (2D and 3D), but they are heavy and inadequate for the resolution of the inverse problems in real time; and depend of the advances in computer technology and computational methods. Given that the simplicity of the adopted mesh and the fastness of calculations (for the studied device the simulation time is lower than 1.09 s in a PC with a CPU frequency of 2 GHz and a RAM of 3 GB), the proposed half analytical method present a very fast tool of simulation in comparison to other methods. Starting from the concept of coupled circuit method we have developed a half analytical method that allows expressing the impedance variation according to the physical and geometrical characteristics of the load and facilitate the resolution of the inverse problems. The comparison of the proposed method results and those of finite element method reveals a great concordance. Furthermore, the obtained results are considered very satisfactory and have conducted to the model validation. One can note that this method is applicable to any axi-symmetric systems and can be adapted for the simulation of three-dimensional configurations.

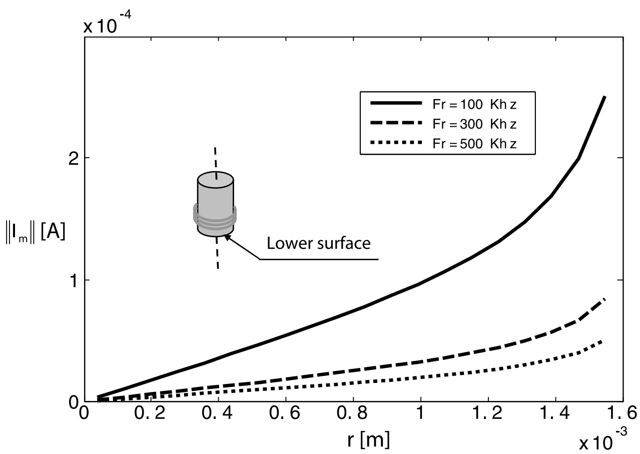

Fig. 4 Fictitious magnetization current, on the lower surface, according the radial axis

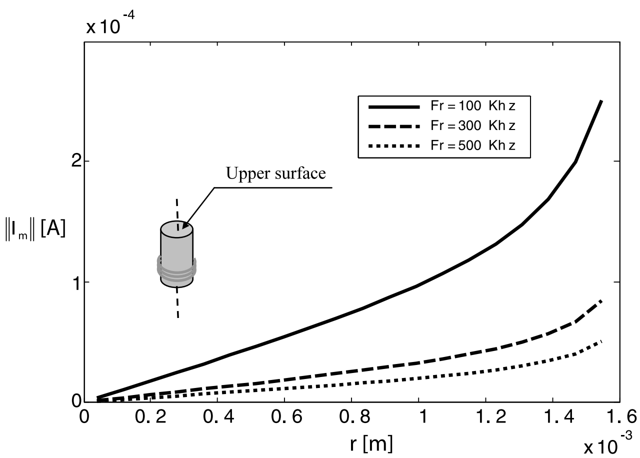

Fig. 5 Fictitious magnetization current, on the upper surface, according the radial axis

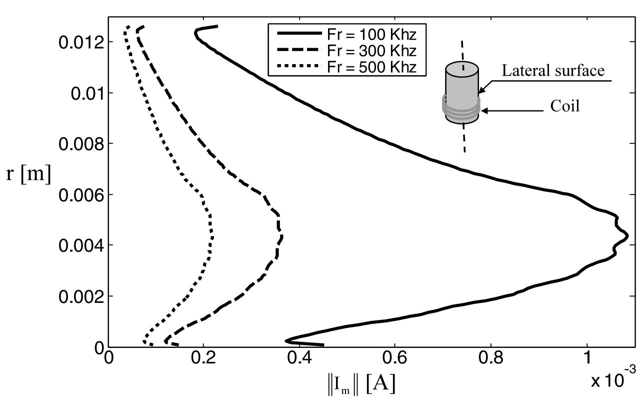

Fig. 6 Evolution of the magnetization fictitious current on the lateral surface

References

1. Maouche, B., Feliachi, M.: A half analytical formulation for the impedance variation in axisymmetrical modeling of eddy current non-destructive testing. Eur. Phys. J. Appl. Phys. **33**, 59–67 (2006)
2. Maouche, B., Feliachi, M.: Analyse de l'effet des courants induits sur l'impédance d'un système électromagnétique alimenté en tension BF ou HF. Utilisation de la méthode des circuits couplés. J. Phys. III **10**, 1967–1973 (1997)
3. Maouche, B., Rezak, A., Feliachi, M.: Semi analytical calculation of the impedance of differential sensor for eddy current non-destructive testing. Nondestruct. Test. Eval. Int. **42**, 573–580 (2009)
4. Bouzidi, A., Maouche, B., Feliachi, M., Berthiau, G.: Pulsed eddy current non-destructive evaluation based on coupled electromagnetic quantities method. Eur. Phys. J. Appl. Phys. **57**, 10601 (2012)
5. Amrane, S., Latreche, M.E.H., Feliachi, M.: Coupled circuits model combined with deterministic and stochastic algorithms for the inductor design. Int. J. Appl. Electromagn. Mech. **32**, 195–206 (2010)
6. Mouhallebi, H., Bouali, F., Feliachi, M.: Use of half analytical method for detection of defects in diet pulses. In: The 15th International Workshop on Electromagnetic Non Destructive Evaluation (ENDE 2010), 13–16 June, Szczecin, Poland (2010)
7. Zerguini, S., Maouche, B., Latreche, M., Feliachi, M.: A coupled fictitious electric circuit's method for impedance of a sensor with ferromagnetic core calculation. application to eddy currents non-destructive testing. Eur. Phys. J. Appl. Phys. **48**, 31202 (2009)
8. Buvat, F., Pichenot, G., Lesselier, D., Lambert, M., Voillaume, H.: A fast model of eddy current ferrite-cored probes for NDE. In: Electromagnetic Non Destructive Evaluation, vol. VIII, pp. 44–51 (2000)
9. Lunin, V.P.: Phenomenological and algorithmic method for the solution of inverse problem of electromagnetic testing. Rus. J. Destruct. Test. **42**, 353–362 (2006)
10. Megali, G., Pellicano, D., Cacciola, M., Calcagno, S., Versaci, M., Morabito, F.C.: EC modeling and enhancement signals in CFRP inspection. Progr. Electromagn. Res. **14**, 45–60 (2010)
11. Cacciola, G., Calcagno, S., Megali, G., Pellican, D., Versaci, M., Morabito, F.C.: Eddy current modeling in composite materials. PIERS Online **5**, 591–595 (2009)
12. Javier, G.-M., Jaime, G.-G., Ernesto, V.-S.: Non-destructive techniques based on eddy current testing. IEEE Sens. J. **11**(3), 2525–2565 (2011)
13. Yating, Y., Pingan, D., Luchuan, X.: Coil impedance calculation of an eddy current sensor by the finite element method. Russ. J. Non destructive Test. **44**(4), 296–302 (2008)
14. Sollier, T., Buvat, F., Pichenot, G., Premel, D.: Eddy current modeling of ferrite-cored probes, application to the simulation of eddy current signals from surface breaking flaws in austenitic steel. In: Proc. 16th World Conf. on NDT, Montreal (2004)
15. Dodd, C.V., Deeds, W.E.: Analytical solutions to eddy-current probe-coil probe problems. J. Appl. Phys. **39**, 2829–2839 (1968)
16. Lu, Y., Bowler, J.R., Theodoulidis, T.P.: An analytical model of a ferrite-cored inductor used as an eddy current probe. J. Appl. Phys. **111**, 103907 (2012)